2019 IEEE 30th Annual International Symposium on Personal, Indoor and Mobile Radio Communications (PIMRC): Track 1: Fundamentals and PHY

Wireless Powered Machine-Type Communication: Energy Minimization via Compressed Transmission

Sheeraz A. Alvi, Xiangyun Zhou, Salman Durrani
Research School of Electrical, Energy and Materials Engineering, The Australian National University, Australia.
Emails: {sheeraz.alvi, xiangyun.zhou, salman.durrani}@anu.edu.au.

***Abstract*—We consider a machine-type communication (MTC) node that is served by a hybrid access point (HAP) which provides RF power transfer to the node and receives data transmission from the node. Due to the lossy wireless medium and limited efficiency of RF energy transducer, the energy cost at the HAP is substantial. To minimize the energy cost while still satisfying the system requirement, the harvested energy at the MTC node must be used efficiently. To this end, we consider that the MTC node employs data compression in order to reduce the energy cost of data transmission. Data compression itself consumes time and energy, which needs to be carefully controlled. Thus, we propose to jointly optimize the harvesting-time, compression and transmission design, to minimize the energy cost of the system under given delay constraint. The proposed scheme achieves up to 19% performance gain, under given system constraints, as compared to optimizing harvesting-time ratio and transmission rate without employing compression.**

I. Introduction

The limited operational time of battery operated wireless machine-type communication (MTC) nodes is a major hurdle in fully realizing the potential of the Internet of Things (IoT) [1]. Radio frequency based energy harvesting (RF-EH) has recently emerged as a promising solution to provide perpetual-lifetime for MTC nodes [2–4], i.e., it may stay operational indefinitely long. In this work, we consider a unified wireless power transfer (WPT) and wireless information transfer (WIT) system. We seek to intelligently design the operation of a MTC node and a hybrid access point (HAP) with an objective to minimize the power transferred by the HAP.

The prior studies have considered the unified WPT and WIT systems from the perspective of RF-EH efficiency [4–7]. The RF-EH is mainly dependent on aspects such as the transmitted power, wireless medium, rectification efficiency, etc. Firstly, the HAP's transmitted power undergoes attenuation due to the fading and pathloss, afterwards the RF-EH circuit's sensitivity threshold (-10 to -30 dBm [4]) further cuts down the received power, and lastly the RF energy transducer harvests energy with a limited efficiency ($< 50\%$ [8]). Consequently, even for a short distance, the HAP spends a substantial amount of energy on WPT process. Therefore, the energy cost of the HAP is an important component to consider for efficient operation of a RF-EH based communication system.

To achieve energy minimization at the HAP, it is critical to minimize the WIT energy cost subject to the system constraints. The existing literature proposes the power-rate adaptation [5–7], [9–11] to minimize the transmission energy cost under the given delay constraint. This approach is only valid when the distance is large and the transmit power dominates the circuit power [6], [7]. In practical RF-EH systems, the distance is very short and thus the circuit power cost cannot be ignored. Thus, decreasing the transmission rate prolongs the transmission time but may not necessarily decrease the transmission energy cost.

Recently, [12] proposed using data compression to minimize the transmission energy cost by reducing the amount of data to transmit. It was shown that jointly optimizing transmission and compression in a traditional non-EH communication system minimized energy consumption significantly (typically over 90%) as compared to optimizing transmission only without compression. Motivated by this potential of data compression to reduce the energy cost, we consider this technique for a wireless powered communication system. In such systems, the time spent on compression (which itself consumes energy [13–15]) must be carefully controlled. To the best of our knowledge, none of the prior works has considered the impact of data compression while devising the WPT and WIT policies for a wireless powered MTC system.

Paper contributions: In this paper, we consider a wireless powered MTC system comprising of a MTC node and a HAP. We employ a *harvest-and-use* strategy, i.e., the HAP first transfers RF power to the MTC node, which then transmits its data to the HAP.

- We propose to jointly optimize energy harvesting, compression and transmission times to minimize the system energy cost, which is injected by the HAP, when only statistical gain is known at the MTC node.
- Our results show that, for practical parameter values, employing and optimizing data compression in a wireless powered MTC system reduces the energy consumption by a further 19%, compared to only optimizing harvesting and transmission times. Specif-

This work was supported by the Australian Research Council's Discovery Project Funding Scheme (Project number DP170100939).

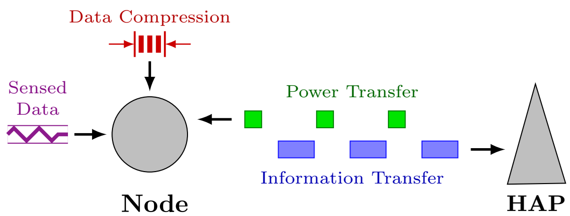

Fig. 1: Illustration of the considered WPCN.

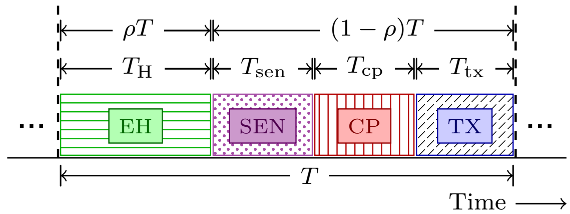

Fig. 2: Energy harvesting (EH), sensing (SEN), compression (CP) and transmission (TX) processing times.

ically, the energy saving is significant when the delay constraint is less stringent.

II. System model

We consider a wireless powered communication system employing a *harvest-and-use* strategy, i.e., the HAP periodically transmits a power beacon and a MTC node harvests RF energy and transmits its sensed data to the HAP, as illustrated in Fig. 1. The system follows a block-wise operation with a block of duration T seconds. Within each time block the MTC node performs four main functions, i.e., (i) energy harvesting, (ii) sensing, (iii) compression and (iv) transmission, as shown in Fig. 2. The energy spent by the MTC node to perform all its operations in a given time block is denoted by E_{MTC}.

Channel model: The MTC node is equipped with an omnidirectional antenna and the HAP is equipped with a directional antenna with gain G. The MTC node and the HAP are located at a distance r. We assume channel reciprocity between WPT and WIT channels [5]. The channel is composed of large scale path loss, with path loss exponent α, and small-scale quasi-static flat Rayleigh fading channel, i.e., the fading channel gain $|h|^2$ remains constant in a given time block and is independently and identically distributed from one time block to the next [5], [16]. We assume the instantaneous channel gain information (CGI) is available only at the HAP [5]. We consider the additive white Gaussian noise for the channel with zero mean and variance σ^2. The noise power density is denoted by N_0.

Energy Harvesting: The HAP is powered by an electrical grid, whereas the MTC node has simple short-term energy storage capability [5], [16]. Hence, we assume that energy accumulation is not possible at the MTC node. During the first T_{H} seconds of a time block, the HAP transmits the power beacon with a fixed transmit power level denoted by P_{PT}, and the MTC node harvests E_{H} units of energy under fading channel gain $|h|^2$, given as

$$E_{\text{H}} = \eta T_{\text{H}} \left(\kappa \frac{|h|^2 P_{\text{PT}}}{r^{\alpha}} - P_{\text{th}} \right)^{+}, \tag{1}$$

where $\kappa = \left(\frac{\nu}{4\pi}\right)^2 G$ is the attenuation factor and ν is the wavelength, $0 \leqslant \eta \leqslant 1$ is the loss in energy transducer during conversion of harvested energy into electrical energy, P_{th} is the RF-EH sensitivity threshold, and $(z)^{+} = \max\{z, 0\}$. Accordingly, the RF-EH circuit can only be activated if the received signal power is greater than a RF-EH sensitivity threshold [16]. The value of the thermal noise power, σ^2, is typically very small, and thus it is not included in the energy harvesting model.

Sensing: We assume the MTC node spends a constant amount of time and energy to acquire a fixed amount of data in each time block [17]. Note that this sensing cost model is generic and may represent any other operation or can even be ignored. Let the time, energy, power spent to sense and generate a fixed data of size D bits is denoted by T_{sen}, E_{sen} and P_{sen}, respectively. E_{sen} is given as

$$E_{\text{sen}} = \vartheta D P_{\text{sen}}, \tag{2}$$

where ϑ is the per bit sensing time.

Compression: Before transmission, the sensed data of size D bits is compressed into D_{cp} bits as per the given compression ratio $\frac{D_{\text{cp}}}{D}$. In this work, we adopt a non-linear compression cost model given in [18] to compute the *compression time*, denoted by T_{cp}, as a function of $\frac{D_{\text{cp}}}{D}$, which is given as

$$T_{\text{cp}} = \frac{\tau D^{\beta+1}}{D_{\text{cp}}^{\beta}} - \tau D, \tag{3}$$

where τ is the per bit processing time and β is the compression algorithm dependent parameter that is proportional to the compression algorithm's complexity. β determines the time cost for achieving a given compression ratio and can be calculated off-line for any specified compression algorithm and given hardware resources. τ depends upon the micro-controller unit (MCU) processing resources and the number of program instructions executed to process 1 bit of data. Note that τ does not represent the compression time per bit. Let P_{cp} denote the power consumed by the MTC node during data compression process. P_{cp} is the same as the power consumed while MCU is processing information, which is predefined.

Transmission: Once the compression process is complete, the MTC node needs to transmit the compressed data, D_{cp}, within the same time block. Let the *transmission time* is denoted by T_{tx}. Thereby, T_{tx} is given as

$$T_{\text{tx}} = \frac{D_{\text{cp}}}{R}, \tag{4}$$

and the transmission rate, R, is given as

$$R = B \log_2 \left(1 + \frac{\kappa |h|^2 P_{\text{IT}}}{\sigma^2 r^{\alpha} \Gamma} \right), \tag{5}$$

where B is the bandwidth of the considered system, P_{IT} is the transmit power level, and Γ characterizes the gap between the achievable rate and the channel capacity due to the use of practical modulation and coding schemes [6].

To compute the data transmission power cost, denoted by P_{tx}, we adopt a practical model as given in [6]. The transmission power cost is composed of two main components, the transmitted power, P_{IT}, and the static communication module circuitry power, denoted by P_{o}, which accounts for digital-to-analog converter, frequency synthesizer, mixer, transmit filter, and antenna circuits, etc. Accordingly, P_{tx} is given as follows

$$P_{\text{tx}} = \frac{P_{\text{IT}}}{\mu} + P_{\text{o}}, \tag{6}$$

where $\mu \in (0, 1]$ is the power amplifier's drain efficiency.

The energy spent by the MTC node to perform all its operations in a given time block is

$$E_{\text{MTC}} = P_{\text{sen}}T_{\text{sen}} + P_{\text{cp}}T_{\text{cp}} + P_{\text{tx}}T_{\text{tx}}. \tag{7}$$

III. Energy Minimization Problem

In this section, we first present the design objective and then formulate the energy minimization problem. Finally, we provide the solution to the problem.

Design Objective: The main problem that we study is to minimize the system energy cost. The target is to optimally utilize the power injected into the system. The MTC node solely relies on the power transferred by the HAP. Thus, the aforementioned objective can be achieved by minimizing the HAP's transmitted energy, $E_{\text{HAP}} = T_{\text{H}}P_{\text{PT}}$, while satisfying the given system constraints. Therefore, we design policies for the RF energy harvesting, compression and transmission processes whilst guaranteeing the desired quality of service (QoS) requirements.

We consider a *harvest-and-use* strategy for energy harvesting and sensed data transmission. Therein, a fraction of the total completion time is spent for energy harvesting operation, which is controlled by the *harvesting-time ratio* denoted by $0 \leqslant \rho \leqslant 1$, such that $T_{\text{H}} = \rho T$. Accordingly, the rest of the time is spent in sensing, compression and transmission processes $T_{\text{sen}} + T_{\text{cp}} + T_{\text{tx}} = (1-\rho)T$, as illustrated in Fig. 2. Moreover, the system requires specific QoS in terms of data reliability and delivery time. This imposes a constraint in terms of the delay bound, which mandates that the cumulative completion time of the MTC node's operations, must meet the deadline, T. Moreover, the system imposes another probabilistic constraint on the successful data delivery. Specifically, the data should be successfully delivered with probability equal to a given value, denoted by δ.

The channel varies independently in different time blocks. In a given time block, if the channel is in deep fade, the required level of energy to transfer, E_{HAP}, would be too high to achieve the given system performance. This high energy cost might be infeasible for a loss tolerant system, a typical case in sensor networks. Moreover, when the channel is in deep fade, the delay bound may also hinder the HAP to transfer the required amount of energy and the MTC node may not be able to complete all of its operations within the given deadline. Also, when the channel is in deep fade, the MTC node would not be able to harvest enough energy to perform its operations within the deadline, referred to as the *energy outage*.

The probability distribution function (pdf) of the CGI, $|h|^2$, is exponentially distributed and is given as

$$f\big(|h|^2\big) \triangleq \frac{1}{\lambda}\exp\Big(-|h|^2\frac{1}{\lambda}\Big), \quad |h|^2 \geqslant 0, \tag{8}$$

where λ is the scale parameter of the pdf.

To minimize HAP's transmitted energy, E_{HAP}, under given data delivery constraint, the best strategy is to exploit the channel diversity in different time blocks. Therein, the system is operated only when the channel gain is larger than a specific value, denoted by Θ, which satisfies the probabilistic data delivery constraint. Accordingly, the value of Θ can be computed using the expression

$$\mathbb{P}\Big\{|h|^2 \geqslant \Theta\Big\} = \delta. \tag{9}$$

The left hand side of (9) represents the complimentary cumulative distribution function (ccdf) for $|h|^2$. For the considered Rayleigh fading channel, the fading power gain, $|h|^2$, is exponentially distributed, which yields

$$1 - \Big[1 - \exp\Big(-\Theta\frac{1}{\lambda}\Big)\Big] = \delta. \tag{10}$$

Solving the above equation for Θ yields

$$\Theta = -\lambda\ln\big(\delta\big).$$

Hence, in a given time block if channel gain is lower than the threshold value, i.e., $|h|^2 < -\lambda\ln(\delta)$, then HAP simply informs the MTC not to perform any of its operations and, for simplicity, we ignore the energy consumed by this action from the HAP.

A. Optimal Design Policies for the MTC Node

When the channel is good enough to preclude the energy outage, i.e., $|h|^2 \geqslant -\lambda\ln(\delta)$, the HAP transmits the power beacon and the MTC node performs all of its operations. This is referred to as an active time block.

Considering the operations at the MTC node, we optimize the harvesting-time, ρ_{MTC}, compressed data size, D_{cp}, and transmitted power, P_{IT}, for a wireless powered MTC node to minimize HAP's transmitted energy, E_{HAP}, under given system constraints. We devise the optimal design considering the worst-case channel condition that is possible in an active time block, i.e., $|h|^2 = -\lambda\ln(\delta)$. It is because the instantaneous CGI is not available at the MTC node, and thus MTC node cannot adapt design parameters to different channel conditions in different time blocks. The worst-case channel based design ensures that the required system performance would be met in all active time blocks using the fixed design parameters.

Minimizing ρ_{MTC} actually minimizes E_{HAP}, because T and P_{PT} are both fixed. Thus, solving the following problem, for given channel realization $|h|^2 = -\lambda \ln(\delta)$, yields optimal MTC node design parameters

$$\begin{aligned} \underset{\rho_{\text{MTC}},\, P_{\text{IT}},\, D_{\text{cp}}}{\text{minimize}} \quad & \rho_{\text{MTC}} \\ \text{subject to} \quad & E_{\text{MTC}}\big(P_{\text{IT}}, D_{\text{cp}}\big) \leqslant -\eta \rho_{\text{MTC}} T \Big(\frac{\kappa \lambda \ln(\delta)}{r^{\alpha} P^{*}_{\text{PT}}} + P_{\text{th}}\Big), \\ & T_{\text{sen}} + T_{\text{cp}} + T_{\text{tx}} \leqslant \big(1 - \rho_{\text{MTC}}\big) T, \\ & 0 \leqslant \rho_{\text{MTC}} \leqslant 1, \;\; P_{\text{IT}} \geqslant 0, \;\; D_{\min} \leqslant D_{\text{cp}} \leqslant D. \end{aligned} \tag{11}$$

where E_{MTC} is given in (7), $D_{\min}$ is the lower bound on the compressed data size and its value depends on the nature of the data and the system application. The first constraint in (11) mandates that the harvested energy by MTC node must be large enough to cover the cumulative energy cost of its operations. The second constraint in (11) mandates that the completion time for all the MTC nodes' operations must meet the delay bound. The remaining constraints reflect practical range of values for harvesting-time ratio, ρ_{MTC}, MTC node's transmitted power, P_{IT}, and the compressed data size, D_{cp}.

The solution to (11) yields optimal MTC node design parameters $\rho^{*}_{\text{MTC}}, P^{*}_{\text{IT}}, D^{*}_{\text{cp}}$ to be used by the MTC node in all active time blocks. Substituting the values of P^{*}_{IT} and D^{*}_{cp} in (7), yields the fixed optimal minimal $E^{*}_{\text{MTC}}\big(P^{*}_{\text{IT}}, D^{*}_{\text{cp}}\big)$ which is used in all active time blocks.

It can be shown that the problem defined in (11) is non-convex, because the first constraint is non-convex in P_{IT}. By substitution of variable $\ln\big(1 - \frac{\kappa \lambda \ln(\delta) P_{\text{IT}}}{\sigma^2 r^{\alpha} \Gamma}\big) = z$ in (7), E_{MTC} can equivalently be defined as

$$E_{\text{MTC}}\big(z, D_{\text{cp}}\big) = P_{\text{sen}} T_{\text{sen}} + P_{\text{cp}} T_{\text{cp}} + \frac{D_{\text{cp}} b}{z} \big(\exp(z) + c\big). \tag{12}$$

where $a = -\frac{\kappa \lambda \ln(\delta)}{\sigma^2 r^{\alpha} \Gamma}$, $b = \frac{\ln(2)}{\mu a B}$, $c = \mu a P_{\text{o}} - 1$.

Let $d = \kappa \lambda \ln(\delta) P_{\text{PT}} r^{-\alpha} + P_{\text{th}}$. Accordingly, the problem defined in (11) can equivalently be given as follows

$$\begin{aligned} \underset{\rho_{\text{MTC}},\, z,\, D_{\text{cp}}}{\text{minimize}} \quad & \rho_{\text{MTC}} \\ \text{subject to} \quad & E_{\text{MTC}}\big(z, D_{\text{cp}}\big) \leqslant -\eta \rho_{\text{MTC}} T d, \\ & T_{\text{sen}} + T_{\text{cp}} + \frac{D_{\text{cp}} \ln(2)}{B z} \leqslant \big(1 - \rho_{\text{MTC}}\big) T, \\ & 0 \leqslant \rho_{\text{MTC}} \leqslant 1, \; z \geqslant \frac{2}{\ln(2)}, \; D_{\min} \leqslant D_{\text{cp}} \leqslant D. \end{aligned} \tag{13}$$

For brevity we omit the proof, however using basic calculus and some algebraic manipulation, it can be shown that the problem in (13) is a convex optimization problem.

The solution to the optimization problem defined in (13) is given by the following theorem.

Theorem 1. *In solving the optimization problem in* (11)*, the optimal* MTC *node's transmitted power is given by*

$$P^{*}_{\text{IT}} = \begin{cases} \widetilde{P}_{\text{IT}}, & \text{if } \mathcal{Q}(\widetilde{P}_{\text{IT}}, \widetilde{D}_{\text{cp}}) < (1 - \widetilde{\rho}_{\text{MTC}}) T. \\ \widehat{P}_{\text{IT}}, & \text{otherwise.} \end{cases} \tag{14}$$

where

$$\widetilde{P}_{\text{IT}} = \frac{1}{a} \exp\Big(\mathrm{W}_0\Big(\exp\big(\ln(c) - 1\big)\Big) + 1\Big) - \frac{1}{a}, \tag{15}$$

where $\mathrm{W}_0(\cdot)$ *is the principle branch of the Lambert* W *function.* $\widehat{P}_{\text{IT}}$ *is given by the solution of the following equation which can be solved numerically using Bisection method*

$$\frac{T_{\text{sen}}}{P^{-1}_{\text{sen}}} + \frac{\tau D^{\beta+1}}{P^{-1}_{\text{cp}} \widehat{D}^{\beta}_{\text{cp}}} + \frac{\widehat{D}_{\text{cp}} b\big(1 + a\widehat{P}_{\text{IT}} + c\big)}{\ln\big(1 + a\widehat{P}_{\text{IT}}\big)} + \frac{\eta T d}{\widehat{\rho}^{-1}_{\text{MTC}}} = \frac{\tau D}{P^{-1}_{\text{cp}}}, \tag{16}$$

and the optimal compression ratio is given by

$$\frac{D^{*}_{\text{cp}}}{D} = \begin{cases} \frac{\widetilde{D}_{\text{cp}}}{D}, & \text{if } \mathcal{Q}(\widetilde{P}_{\text{IT}}, \widetilde{D}_{\text{cp}}) < (1 - \widetilde{\rho}_{\text{MTC}}) T. \\ \frac{\widehat{D}_{\text{cp}}}{D}, & \text{otherwise.} \end{cases} \tag{17}$$

and the optimal harvesting-time ratio is given by

$$\rho^{*}_{\text{MTC}} = \begin{cases} \widetilde{\rho}_{\text{MTC}}, & \text{if } \mathcal{Q}(\widetilde{P}_{\text{IT}}, \widetilde{D}_{\text{cp}}) < (1 - \widetilde{\rho}_{\text{MTC}}) T. \\ \widehat{\rho}_{\text{MTC}}, & \text{otherwise.} \end{cases} \tag{18}$$

where

$$\frac{\widetilde{D}_{\text{cp}}}{D} = \left(\frac{\tau \beta P_{\text{cp}} \ln(1 + a\widetilde{P}_{\text{IT}})}{b\big(1 + a\widetilde{P}_{\text{IT}}\big) + bc}\right)^{\frac{1}{\beta+1}}, \tag{19}$$

$$\frac{\widehat{D}_{\text{cp}}}{D} = \left(\frac{\tau \beta \big(T^{-1} \widehat{\Lambda}^{-1}_{1} + \eta d - P_{\text{cp}}\big) \ln(1 + a\widehat{P}_{\text{IT}})}{\frac{\widehat{\Lambda}^{-1}_{1} \ln(2)}{TB} + \frac{\eta d \ln(2)}{B} - b(1 + a\widehat{P}_{\text{IT}}) - bc}\right)^{\frac{1}{\beta+1}}, \tag{20}$$

$$\widetilde{\rho}_{\text{MTC}} = \frac{1}{\eta T d}\left(\frac{\tau D}{P^{-1}_{\text{cp}}} - \frac{T_{\text{sen}}}{P^{-1}_{\text{sen}}} - \frac{\tau D^{\beta+1}}{P^{-1}_{\text{cp}} \widetilde{D}^{\beta}_{\text{cp}}} - \frac{\widetilde{D}_{\text{cp}} b(1 + a\widetilde{P}_{\text{IT}} + c)}{\ln\big(1 + a\widetilde{P}_{\text{IT}}\big)}\right), \tag{21}$$

$$\widehat{\rho}_{\text{MTC}} = \frac{1}{T}\left(T - T_{\text{sen}} - \frac{\tau D^{\beta+1}}{\widehat{D}^{\beta}_{\text{cp}}} + \tau D - \frac{\widehat{D}_{\text{cp}} \ln(2)}{B \ln\big(1 + a\widehat{P}_{\text{IT}}\big)}\right). \tag{22}$$

$$\mathcal{Q}(\widetilde{P}_{\text{IT}}, \widetilde{D}_{\text{cp}}) \triangleq T_{\text{sen}} + \frac{\tau D^{\beta+1}}{\widetilde{D}^{\beta}_{\text{cp}}} - \tau D + \frac{B^{-1} \widetilde{D}_{\text{cp}} \ln(2)}{\ln\big(1 + a\widetilde{P}_{\text{IT}}\big)}, \tag{23}$$

$$\widehat{\Lambda}_1 = \frac{T^{-1} B^{-1} \ln(2)}{b\big(\ln\big(1 + a\widehat{P}_{\text{IT}}\big) - 1\big)\big(1 + a\widehat{P}_{\text{IT}}\big) - bc - \eta d B^{-1} \ln(2)}. \tag{24}$$

Proof: The proof is provided in Appendix A. ■

Following remark discusses an insight from Theorem 1.

Remark 1. $\widetilde{P}_{\text{IT}}$*,* $\widetilde{D}_{\text{cp}}$*,* $\widetilde{\rho}_{\text{MTC}}$ *provide an upper bound on the HAP's energy cost in any active time block,* $\rho^{*}_{\text{MTC}} T P_{\text{PT}}$*, and are optimal design parameters when all constraints in* (11) *are slack, i.e.,* $\mathcal{Q}(\widetilde{P}_{\text{IT}}, \widetilde{D}_{\text{cp}}) < (1 - \widetilde{\rho}_{\text{MTC}}) T$*, except the first constraint. On the other hand,* $\widehat{P}_{\text{IT}}$*,* $\widehat{D}_{\text{cp}}$*,* $\widehat{\rho}_{\text{MTC}}$ *are optimal design parameters, when all constraints in* (11) *are slack except for the first and second constraint.*

B. Optimal Design Policies for the HAP

Finally, we can relate the design for the MTC node, given in Theorem 1, to determine the HAP's optimal design. The MTC node employs a fixed harvesting-time ratio ρ^{*}_{MTC}, defined in (18), in all active time blocks. ρ^{*}_{MTC} is determined based on the worst-case channel condition due to the unavailability of instantaneous CGI at the MTC node. However, the instantaneous CGI is available at the HAP, thus it can adapt the harvesting-time for different channel conditions in different active time blocks. Accordingly, the actual harvesting-time used by the HAP

TABLE I: System parameter values.

Name	Sym.	Value	Name	Sym.	Value	Name	Sym.	Value
RF-EH sensitivity threshold	P_{th}	-30 dBm	Energy transducer efficiency	η	0.5	Pathloss exp.	α	3
Sensing power cost	P_{sen}	70 mW	Power amplifier efficiency	μ	0.35	Antenna gain	G	10
Compression power cost	P_{cp}	24 mW	Compression cost parameter	β	5	Bandwidth	B	2 MHz
HAP transmitted power	P_{PT}	40 dBm	Per bit processing time	τ	3.9 ns/b	Noise density	N_0	-174 dBm
Radio circuitry power	P_{o}	82.5 mW	CGI's *pdf* scale parameter	λ	1	Data size	D	200 bits
Data delivery probability	δ	0.80	Per bit sensing time	ϑ	37 ns/b	Distance	r	10 m
Min. compressed data size	D_{min}	$0.5\times D$	Modulation gap parameter	Γ	0 dB	Wavelength	ν	0.125 m

to transfer power is given by $\rho^*_{\text{HAP}}T$, where

$$\rho^*_{\text{HAP}}\left(|h|^2\right) \triangleq \frac{E^*_{\text{MTC}}\left(P^*_{\text{IT}}, D^*_{\text{cp}}\right)}{\eta T\left(\kappa|h|^2 r^{-\alpha}P_{\text{PT}}+P_{\text{th}}\right)} \leqslant \rho^*_{\text{MTC}}. \quad (25)$$

where $|h|^2 \geqslant -\lambda \ln\left(\delta\right)$ is the instantaneous channel gain in an active time block. Note that the actual harvesting-time, ρ^*_{HAP}, is almost always less than ρ^*_{MTC}.

The minimal HAP's transmitted energy is given as

$$E^*_{\text{HAP}} = \rho^*_{\text{HAP}}TP_{\text{PT}}. \quad (26)$$

IV. Numerical Results

In this section, we present the numerical results to observe the performance of the proposed scheme. Unless specified otherwise, the values adopted for the system parameters are shown in Table I. Note that we assume realistic values, consistent with prior works, for EH [9] and sensing, compression, transmission operations.

Baseline scheme: To illustrate the advantage of joint optimization of harvesting-time ratio, compression and transmission rate, we also consider a baseline scheme which minimizes E_{HAP} by optimizing harvesting-time ratio and transmission rate only (no data compression is employed) whilst satisfying the system constraints. This problem can be given by substituting $D_{\text{cp}} = D$ in (11). The optimal MTC node's transmitted power, denoted by $P^*_{\text{IT,nc}}$, and harvesting-time ratio, denoted by $\rho^*_{\text{MTC,nc}}$, for the baseline scheme can be obtained using Proposition 1.

Proposition 1. *The optimal* MTC *node's transmitted power, without employing compression, is given by*

$$P^*_{\text{IT,nc}} = \begin{cases} \widetilde{P}_{\text{IT,nc}}, & \text{if } T_{\text{sen}}+\frac{B^{-1}D\ln(2)}{\ln\left(1+a\widetilde{P}_{\text{IT}}\right)} < \frac{1-\widetilde{\rho}_{\text{MTC,nc}}}{T^{-1}}. \\ \widehat{P}_{\text{IT,nc}}, & \text{otherwise.} \end{cases} \quad (27)$$

where

$$\widetilde{P}_{\text{IT,nc}} = \frac{1}{a}\exp\left(\text{W}_0\Big(\exp\left(\ln(c)-1\right)\Big)+1\right)-\frac{1}{a}, \quad (28)$$

$$\widehat{P}_{\text{IT,nc}} = \frac{1}{a}\exp\left(\frac{u}{v}-\text{W}_0\left(-\frac{bD}{\eta d v}\exp\left(\frac{u}{v}\right)\right)\right)-\frac{1}{a}, \quad (29)$$

where $u = \frac{cbD}{\eta d} - \frac{D\ln(2)}{B}$ *and* $v = T_{\text{sen}} - \frac{T_{\text{sen}}P_{\text{sen}}}{\eta d} - T$. *The optimal harvesting-time ratio is given by*

$$\rho^*_{\text{MTC,nc}} = \begin{cases} \widetilde{\rho}_{\text{MTC,nc}}, & \text{if } T_{\text{sen}}+\frac{B^{-1}D\ln(2)}{\ln\left(1+a\widetilde{P}_{\text{IT}}\right)} < \frac{1-\widetilde{\rho}_{\text{MTC,nc}}}{T^{-1}}. \\ \widehat{\rho}_{\text{MTC,nc}}, & \text{otherwise.} \end{cases} \quad (30)$$

where

$$\widetilde{\rho}_{\text{MTC,nc}} = -\frac{1}{\eta T d}\left(T_{\text{sen}}P_{\text{sen}} + \frac{Db(1+a\widetilde{P}_{\text{IT,nc}}+c)}{\ln(1+a\widetilde{P}_{\text{IT,nc}})}\right), \quad (31)$$

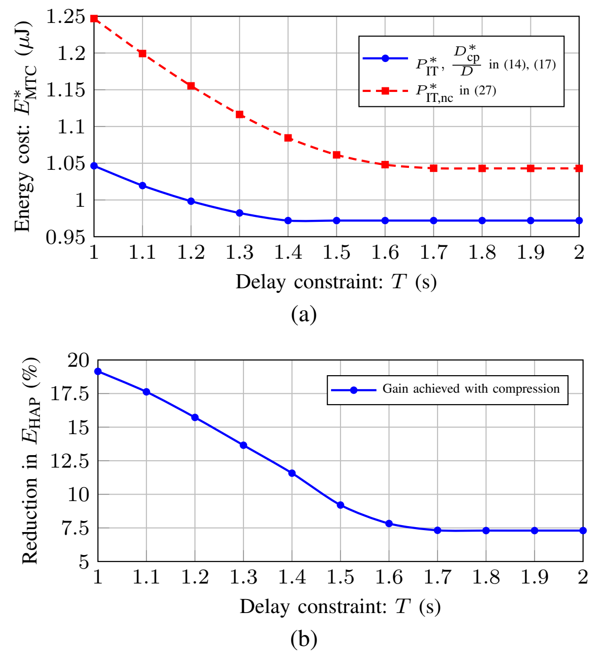

Fig. 3: (a) MTC node's energy cost vs. delay, and (b) performance gain achieved by HAP through compression.

$$\widehat{\rho}_{\text{MTC,nc}} = \frac{1}{T}\left(T - T_{\text{sen}} - \frac{D\ln(2)}{B\ln(1+a\widehat{P}_{\text{IT,nc}})}\right). \quad (32)$$

Proof: The proof follows similar steps as the proof of Theorem 1, substituting $D_{\text{cp}} = D$. For brevity, we omit it. ■

Note that, E^*_{HAP} is now only proportional to E^*_{MTC}, since all other parameters in (25) and (26) are same for both the schemes. Thus, we focus on the MTC node's performance.

Advantage of Proposed Scheme: Fig. 3 plots the MTC node's energy cost, E_{MTC}, versus the delay constraint, T, for system parameters in Table I. E_{MTC} is plotted using the optimal MTC node design parameters for the proposed scheme, when it employs data compression, and for the baseline scheme, when compression is not employed.

The MTC node's energy cost, E_{MTC}, is fixed for all active time-blocks, however the energy of the HAP is different for different active time block. Nevertheless, the HAP enjoys a constant performance gain (decrease in its energy cost) when the MTC node employs data compression. We can see that the gain compared to the baseline scheme is significant - up to 19% for the considered

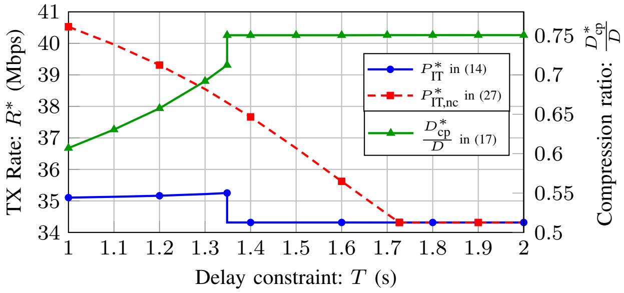

Fig. 4: MTC node's optimal transmission rate and compression ratio, vs. the delay bound.

range of delay constraint. This shows the advantage of employing compression and jointly optimizing harvesting-time ratio, compression and transmission. In both the cases, the performance gain straightens out when the upper-bound on the transmission time is achieved. This bound means that increasing the transmission time, by reducing the transmission rate further, would not decrease the energy cost of the MTC node.

Impact of Delay Constraint: Fig. 4 plots the transmission rate and compression ratio, and the MTC node's operational timing, versus the delay constraint, T, for system parameters in Table I. We can see that the transmission rate requirement is significantly higher for the baseline scheme. However, in the proposed scheme the rate is almost constant and the compression ratio is adapted to the delay constant. Once the upper-bound on the transmission time is reached, both schemes do not need to change the design parameters to adapt to the delay constraint. Thanks to the data compression, this upper-bound value is relatively smaller for the proposed scheme. Thus, employing compression notably decreases the transmission rate requirement at the MTC node.

For the proposed scheme, the timing information for different operations of the MTC node in an active time block is given in Table II. The percentage of time dedicated for the power transfer operation is $99\%, 93\%, 80\%$, for delay bound values $1\,\text{s}, 1.5\,\text{s}, 2\,\text{s}$, respectively. Hence, due to the inherent limited efficiency of the RF-EH process, specifically when the delay constraint is stringent, almost all the active time-block is dedicated for the power transfer operation. On the other hand, the time available for the MTC node to perform its operations is $20\,\mu\,\text{s}, 101\,\text{ms}, 391\,\text{ms}$, for delay bound values $1\,\text{s}, 1.5\,\text{s}, 2\,\text{s}$, respectively. Note that only $97.78\%, 0.014\%, 0.0037\%$, of the available time is actually spent by the MTC node, for delay bound values $1\,\text{s}, 1.5\,\text{s}, 2\,\text{s}$, respectively. Thus, the actual spent time is very small and most of the time is spent on the RF-EH process. This is because, the design considers worst-case channel due to the lack of instantaneous CGI at the MTC node. For practical parameter values, the results in Table II confirm the feasibility and provide insights into the actual operation of a RF-EH powered MTC node.

TABLE II: MTC node's operational timing vs. delay bound.

T(s)	$\rho^*_{\text{MTC}}T$(s)	$T_{\text{sen}}(\mu s)$	$T^*_{\text{cp}}(\mu s)$	$T^*_{\text{tx}}(\mu s)$	$T_{\text{sen}}+T^*_{\text{cp}}+T^*_{\text{tx}}(\mu s)$
1	0.999	7.400	8.696	3.458	19.555
1.5	1.399	7.400	2.504	4.373	14.277
2	1.609	7.400	2.502	4.374	14.275

V. Conclusion

We investigated the joint WPT and WIT policies, employing data compression, to minimize the energy transferred by the HAP under given system constraints. For practical parameter values, the joint optimization performs significantly better than only optimizing harvesting-time ratio and transmission rate without compression. Specifically, the gain is relatively large, up to 19%, when the delay constraint is stringent.

Appendix A
Proof of Theorem 1

Lagrangian function for (13) can be given as in (33) shown at the top of the next page, where $\Lambda_i \in \mathbf{\Lambda} = \{\Lambda_1, \Lambda_2, \Lambda_3, \Lambda_4\}$ is the Lagrangian multiplier associated with the ith constraint.

The Karush-Kuhn-Tucker (KKT) conditions for (13) are

$$\begin{aligned}&\Lambda_1\Big(\frac{D_{\text{cp}}b}{z}\big(\exp(z)+c\big)+\frac{\tau D^{\beta+1}}{D_{\text{cp}}^{\beta}P_{\text{cp}}^{-1}}-\tau DP_{\text{cp}}+\eta\rho_{\text{MTC}}Td\\&+P_{\text{sen}}T_{\text{sen}}\Big)=0,\ \ \Lambda_6(D_{\min}-D_{\text{cp}})=0,\ \ \Lambda_7(D_{\text{cp}}-D)=0,\\&\Lambda_2\Big(T_{\text{sen}}+\frac{\tau D^{\beta+1}}{D_{\text{cp}}^{\beta}}-\tau D+\frac{\ln(2)}{BzD_{\text{cp}}^{-1}}-T+\rho_{\text{MTC}}T\Big)=0,\\&-\Lambda_3\rho_{\text{MTC}}=0,\ \ \Lambda_4(\rho_{\text{MTC}}-1)=0,\ \ \Lambda_5\Big(\frac{2}{\ln(2)}-z\Big)=0,\end{aligned} \tag{34a}$$

$$\Big[\frac{\partial\mathcal{L}}{\partial\rho_{\text{MTC}}}\ \frac{\partial\mathcal{L}}{\partial z}\ \frac{\partial\mathcal{L}}{\partial D_{\text{cp}}}\Big]^{\top}=[0\ 0\ 0]^{\top}. \tag{34b}$$

where $[\cdot]^{\top}$ is the transpose operator.

From (33), taking and setting $\frac{\partial\mathcal{L}}{\partial\rho_{\text{MTC}}}=0$ we get

$$1+\Lambda_1\eta Td+\Lambda_2T-\Lambda_3=0. \tag{35}$$

From (33), taking and setting $\frac{\partial\mathcal{L}}{\partial z}=0$ we get

$$\frac{\Lambda_1D_{\text{cp}}b}{z^2}\Big((z-1)\exp(z)-c\Big)-\frac{\Lambda_2\ln(2)}{Bz^2D_{\text{cp}}^{-1}}-\Lambda_5=0. \tag{36}$$

From (33), taking and setting $\frac{\partial\mathcal{L}}{\partial D_{\text{cp}}}=0$ we get

$$\begin{aligned}&\Lambda_1\big(-\tau\beta D^{\beta+1}D_{\text{cp}}^{-\beta-1}P_{\text{cp}}+bz^{-1}\big(\exp(z)+c\big)\big)+\\&\Lambda_2\Big(-\tau\beta D^{\beta+1}D_{\text{cp}}^{-\beta-1}+\frac{\ln(2)}{Bz}\Big)-\Lambda_6+\Lambda_7=0.\end{aligned} \tag{37}$$

From (34a) we know either Λ_i is zero or the associated constraint function is zero for any given i. First consider that only Λ_1 exists. Accordingly, solving (35) for Λ_1 and substituting its value in (36) and solving for z yields

$$\tilde{z}=\mathrm{W}_0\big(\exp\big(\ln(c)-1\big)\big)+1, \tag{38}$$

where $\mathrm{W}_0(\cdot)$ is the Lambert function's principle branch.

$$\begin{aligned}\mathcal{L}(\rho_{\text{MTC}}, z, D_{\text{cp}}, \mathbf{\Lambda}) = \rho_{\text{MTC}} + \Lambda_1\Big(P_{\text{sen}}T_{\text{sen}} + \frac{\tau D^{\beta+1}P_{\text{cp}}}{D_{\text{cp}}^{\beta}} - \tau D P_{\text{cp}} + \frac{b(\exp(z)+c)}{z\widehat{D}_{\text{cp}}^{-1}} + \eta\rho_{\text{MTC}}Td\Big) - \Lambda_3\rho_{\text{MTC}} + \Lambda_4(\rho_{\text{MTC}}-1)\\ + \Lambda_2\Big(T_{\text{sen}} + \frac{\tau D^{\beta+1}}{D_{\text{cp}}^{\beta}} - \tau D + \frac{\ln(2)}{BzD_{\text{cp}}^{-1}} - T + \rho_{\text{MTC}}T\Big) + \Lambda_5\Big(\frac{2}{\ln(2)} - z\Big) + \Lambda_6(D_{\min} - D_{\text{cp}}) + \Lambda_7(D_{\text{cp}} - D),\end{aligned} \tag{33}$$

Substituting z from (38) into (37) yields

$$\widetilde{D}_{\text{cp}} = D\Big(\frac{\tau\beta P_{\text{cp}}\,\tilde{z}}{b\exp(\tilde{z}) + bc}\Big)^{\frac{1}{\beta+1}}. \tag{39}$$

Since, $\Lambda_1 \neq 0$, thereby, from (34a), we have

$$\frac{\eta Td}{\rho_{\text{MTC}}^{-1}} = \frac{\tau D}{P_{\text{cp}}^{-1}} - \frac{T_{\text{sen}}}{P_{\text{sen}}^{-1}} - \frac{\tau D^{\beta+1}}{P_{\text{cp}}^{-1}\,\widetilde{D}_{\text{cp}}^{\beta}} - \frac{\widetilde{D}_{\text{cp}}b}{\tilde{z}}\big(\exp(\tilde{z})+c\big). \tag{40}$$

Solving (40) for ρ_{MTC} yields its value given as follows

$$\widetilde{\rho}_{\text{MTC}} = \frac{1}{\eta Td}\Big(\frac{\tau D}{P_{\text{cp}}^{-1}} - \frac{T_{\text{sen}}}{P_{\text{sen}}^{-1}} - \frac{\tau D^{\beta+1}}{P_{\text{cp}}^{-1}\,\widetilde{D}_{\text{cp}}^{\beta}} - \frac{\exp(\tilde{z})+c}{\tilde{z}b^{-1}\,\widetilde{D}_{\text{cp}}^{-1}}\Big). \tag{41}$$

It can be shown that $\tilde{z}$, $\widetilde{D}_{\text{cp}}$, $\widetilde{\rho}_{\text{MTC}}$ satisfy all the KKT conditions, thus are optimal for the problem in (13), when all constraints in (13) are slack, except the first constraint.

Now consider that Λ_1, Λ_2 exist and $\Lambda_3, \Lambda_4, \Lambda_5, \Lambda_6, \Lambda_7$ do not exist. Accordingly, solving (35) for Λ_2 yields

$$\widehat{\Lambda}_2 = -T^{-1} - \Lambda_1\eta d. \tag{42}$$

Substituting Λ_2 from (42) into (36) yields

$$\widehat{\Lambda}_1 = \frac{T^{-1}B^{-1}\ln(2)}{b(z-1)\exp(z) - bc - \eta dB^{-1}\ln(2)}. \tag{43}$$

Substituting the value of Λ_2 from (42) into (37) and solving for D_{cp} yields its value given as follows

$$\widehat{D}_{\text{cp}} = D\left(\frac{z\tau\beta\big(T^{-1}\widehat{\Lambda}_1^{-1} + \eta d - P_{\text{cp}}\big)}{\frac{\ln(2)}{\widehat{\Lambda}_1TB} + \frac{\eta d\ln(2)}{B} - b\exp(z) - bc}\right)^{\frac{1}{\beta+1}}, \tag{44}$$

where $\widehat{\Lambda}_1$ is a function of z and is defined in (43).

Since, $\Lambda_2 \neq 0$, accordingly, from (34a), we have

$$T_{\text{sen}} + \tau D^{\beta+1}\,\widehat{D}_{\text{cp}}^{-\beta} - \tau D + \frac{\widehat{D}_{\text{cp}}\ln(2)}{Bz} - T + \rho_{\text{MTC}}T = 0. \tag{45}$$

Solving (45) for ρ_{MTC} yields its value given as follows

$$\widehat{\rho}_{\text{MTC}} = \frac{1}{T}\Big(T - T_{\text{sen}} - \tau D^{\beta+1}\,\widehat{D}_{\text{cp}}^{-\beta} + \tau D - \frac{\widehat{D}_{\text{cp}}\ln(2)}{Bz}\Big). \tag{46}$$

Also, $\Lambda_1 \neq 0$, thereby, from (34a), we have

$$\frac{T_{\text{sen}}}{P_{\text{sen}}^{-1}} + \frac{\tau D^{\beta+1}}{P_{\text{cp}}^{-1}\,\widehat{D}_{\text{cp}}^{\beta}} - \frac{\tau D}{P_{\text{cp}}^{-1}} + \frac{b(\exp(z)+c)}{z\,\widehat{D}_{\text{cp}}^{-1}} + \frac{\eta\,\widehat{\rho}_{\text{MTC}}}{(Td)^{-1}} = 0. \tag{47}$$

Numerically solving (47) for z and substituting this value in (42), (43), (44), (46) yields the values of $\widehat{\Lambda}_2$, $\widehat{\Lambda}_1$, $\widehat{D}_{\text{cp}}$ and $\widehat{\rho}_{\text{MTC}}$, respectively. It can be shown that $\widehat{D}_{\text{cp}}$, $\widehat{\rho}_{\text{MTC}}$, $\widehat{z}$ satisfy all the KKT conditions and thus are optimal for (13), when all constraints are slack except the first and second constraint. All other cases for the lagrange multipliers violate one or more KKT conditions.

The problem in (13) is equivalent to (11), thus the optimal values of D_{cp}, ρ_{MTC}, P_{IT}, for both cases can be obtained by substituting $z = \ln\big(1 - \frac{\kappa\lambda\ln(\delta)P_{\text{IT}}}{\sigma^2r^{\alpha}\Gamma}\big)$ in (42), (43), (44), (46), which will minimize the objective function in (11).

REFERENCES

[1] Z. Dawy, W. Saad, A. Ghosh, J. G. Andrews, and E. Yaacoub, "Toward massive machine type cellular communications," *IEEE Wireless Commun.*, vol. 24, no. 1, pp. 120–128, Feb. 2017.

[2] S. Bi, C. K. Ho, and R. Zhang, "Wireless powered communication: opportunities and challenges," *IEEE Commun. Mag.*, vol. 53, no. 4, pp. 117–125, Apr. 2015.

[3] D. N. K. Jayakody, J. Thompson, S. Chatzinotas, and S. Durrani, *Wireless Information and Power Transfer: A New Paradigm for Green Communications*. Springer International Publishing AG, 2017.

[4] X. Lu, P. Wang, D. Niyato, D. I. Kim, and Z. Han, "Wireless networks with RF energy harvesting: A contemporary survey," *IEEE Commun. Surveys Tuts.*, vol. 17, no. 2, pp. 757–789, Nov. 2015.

[5] H. Ju and R. Zhang, "Throughput maximization in wireless powered communication networks," *IEEE Trans. Wireless Commun.*, vol. 13, no. 1, pp. 418–428, Jan. 2014.

[6] Q. Wu, M. Tao, D. W. K. Ng, W. Chen, and R. Schober, "Energy-efficient resource allocation for wireless powered communication networks," *IEEE Trans. Wireless Commun.*, vol. 15, no. 3, pp. 2312–2327, Mar. 2016.

[7] X. Lin, L. Huang, C. Guo, P. Zhang, M. Huang, and J. Zhang, "Energy-efficient resource allocation in TDMS-based wireless powered communication networks," *IEEE Commun. Lett.*, vol. 21, no. 4, pp. 861–864, Apr. 2017.

[8] S. Hemour and K. Wu, "Radio-frequency rectifier for electromagnetic energy harvesting: development path and future outlook," *Proc. of the IEEE,*, vol. 102, no. 11, pp. 1667–1691, Nov. 2014.

[9] W. Liu, X. Zhou, S. Durrani, H. Mehrpouyan, and S. D. Blostein, "Energy harvesting wireless sensor networks: Delay analysis considering energy costs of sensing and transmission," *IEEE Trans. Wireless Commun.*, vol. 15, no. 7, pp. 4635–4650, Jul. 2016.

[10] M. A. Antepli, E. Uysal-Biyikoglu, and H. Erkal, "Optimal packet scheduling on an energy harvesting broadcast link," *IEEE J. Sel. Areas Commun.*, vol. 29, no. 8, pp. 1721–1731, Sep. 2011.

[11] M. Gregori and M. Payaro, "Energy-efficient transmission for wireless energy harvesting nodes," *IEEE Trans. Wireless Commun.*, vol. 12, no. 3, pp. 1244–1254, Mar. 2013.

[12] S. Alvi, X. Zhou, and S. Durrani, "Optimal compression and transmission rate control for node-lifetime maximization," *IEEE Trans. Wireless Commun.*, vol. 17, no. 11, pp. 7774–7788, Nov. 2018.

[13] C. M. Sadler and M. Martonosi, "Data compression algorithms for energy-constrained devices in delay tolerant networks," in *Proc. SENSYS*. ACM, Nov. 2006, pp. 265–278.

[14] T. Srisooksai, K. Keamarungsi, P. Lamsrichan, and K. Araki, "Practical data compression in wireless sensor networks: A survey," *Journal of Network and Computer Applications*, vol. 35, no. 1, pp. 37 – 59, 2012.

[15] Y. Wang, D. Wang, X. Zhang, J. Chen, and Y. Li, "Energy-efficient image compressive transmission for wireless camera networks," *IEEE Sensors J.*, vol. 16, no. 10, pp. 3875–3886, May 2016.

[16] T. Q. Wu and H. C. Yang, "On the performance of overlaid wireless sensor transmission with RF energy harvesting," *IEEE J. Sel. Areas Commun.*, vol. 33, no. 8, pp. 1693–1705, Aug. 2015.

[17] S. Mao, M. H. Cheung, and V. W. S. Wong, "Joint energy allocation for sensing and transmission in rechargeable wireless sensor networks," *IEEE Trans. Veh. Technol.*, vol. 63, no. 6, pp. 2862–2875, Jul. 2014.

[18] M. Tahir and R. Farrell, "A cross-layer framework for optimal delay-margin, network lifetime and utility tradeoff in wireless visual sensor networks," *Ad Hoc Networks*, vol. 11, no. 2, pp. 701–711, Mar. 2013.